Recent Challenges in SMR Rod Bundle Critical Heat Flux Prediction

Nhan-Hien Hoang[a,*], Seong-Su Jeon[a], Ju-Yeop Park[b]
[a] *FNC Technology Co. Ltd. 13 Heungdeok 1-ro, Giheung-gu, Yongin-si, Gyeonggi-do, 16954, Republic of Korea*
[b] *Korea Institute of Nuclear Safety, 62 Kwahak-ro, Yuseong-gu, Daejeon-si, 34142, Republic of Korea*
E-mail: hnhien@fnctech.com

***Keywords :** *CHF, SMR, rod bundle, low-pressure low flow, homogeneous nucleation.*

1. Introduction

Critical heat flux (CHF) is a crucial factor in the design and operation of light water reactors (LWRs). The CHF phenomenon not only limits the available power during normal operating conditions but also defines the limit for safety margins during accident conditions. Great progress has been achieved on this challenging topic [1]. Besides, new considerations have emerged on the rod bundle CHF regarding the recent development of advanced small modular reactors (SMRs).

Some critical issues were reported on the SMR rod bundle CHF concerning the special characteristics of SMR designs [2]. The SMRs use shorter fuel bundles with non-uniform heating and higher axial power peaking, the Soluble-Boron Free design for eliminating its negative drawbacks, and a long large upper plenum of unheated coolant above the active core for enhancing the driving force of natural circulation (e.g., in SMART reactor). Especially, the SMRs have a broad range of concerned thermal-hydraulics conditions from natural to forced convection, and their response to power change is faster due to their small size. Hence, there is a large deviation in the CHF mechanism from the traditional LWRs regarding low-pressure low-flow (LPLF) conditions, flow instability, reflood quenching, upstream burnout, and uncertain effects of the mixing vane and unheated solid wall. As reported, the conventional PWR CHF correlations overpredicted the SMR rod bundle CHF data up to 258 % [3].

Due to the current rise of the SMRs, this study attempts to reevaluate the SMR rod bundle CHF issues by performing MARS-KS/CTF analyses for a conceptual 5×5 rod bundle test. The LPLF CHF was also checked through an example analysis of the SMARTsafety injection (SI) break using the MARS-KS system analysis code. This study is expected to output a better understanding of the SMR rod bundle CHF to support the design and operation of the SMRs.

2. Rod bundle CHF flow pattern

Once the rate of heat removal, which is governed by flow dynamics, is insufficient to remove the inputted heat, CHF will occur. Le Corre et al. (2010) analyzed the existing CHF visualization data and found that flow pattern at the CHF condition can be one of three common ones, i.e., bubbly, vapor clot, and slug, which were mapped into three visible regions in a Weber–quality map [4]. The boundary between the bubbly and vapor clot regions shifts toward higher Weber number and/or lower quality at higher pressure due to a decrease in Kelvin-Helholtz critical length with pressure. However, no criteria were proposed for such boundaries.

Liu and Nariai (2005) analyzed the existing CHF data and divided them into two groups of flow patterns, conventional and homogeneous nucleation (HN) flow patterns (Fig. 1) [5]. They indicated that under extreme conditions such as extremely high mass flux (G), extremely high pressure (P), or low L/D, the CHF can occur without the establishment of the net vapor generation (NVG) point if the heat flux required for the NVG (q_{NVG}) is greater than the heat flux required for HN (q_{HN}). The wall temperature will exceed the HN temperature leading to the explosive generation of molecular vapor bubbles, and significant accumulation of such bubbles will trigger the CHF. About 17 percent of 2656 evaluated data points followed the HN flow pattern.

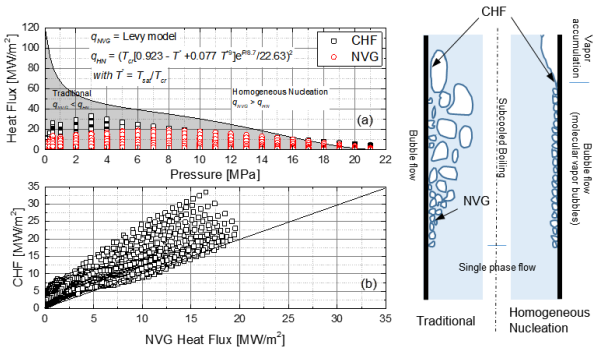

Fig. 1. Evaluation of the 2006 CHF lookup table [6]

Bao and co-workers [1-3] insisted that CHF encountered in SMR rod bundles under the LPLF high-quality condition follows the HN-type CHF. However, our evaluation of the 2006 CHF lookup table [6], which covers the entire SMR operating condition, showed that most of the CHF points lie below the HN heat flux line and above the NVG heat fluxes (Fig. 1). In other words, the HN flow pattern is rarely encountered under the CHF condition. Instead, the NVG point is often established before the occurrence of the CHF (i.e., traditional type).

3. Analysis of conceptual 5×5 rod bundle test

Several factors influence the SMR rod bundle CHF, such as non-uniform heating, reflood quenching, flow mixing caused by mixing vane, and even flow instability under the LPLF condition. To examine these factors, a conceptual rod bundle problem was constructed based on the CE 5×5 rod bundle test (Fig. 2). A 5×5 rod bundle of 2 m length is connected to two unheated volumes at the bottom and the top to simulate the SMART reactor core. The ratio of the height of each part is 1/1 while the volume is scaled down by 1/405. The test was analyzed using the MARS-KS/CTF code.

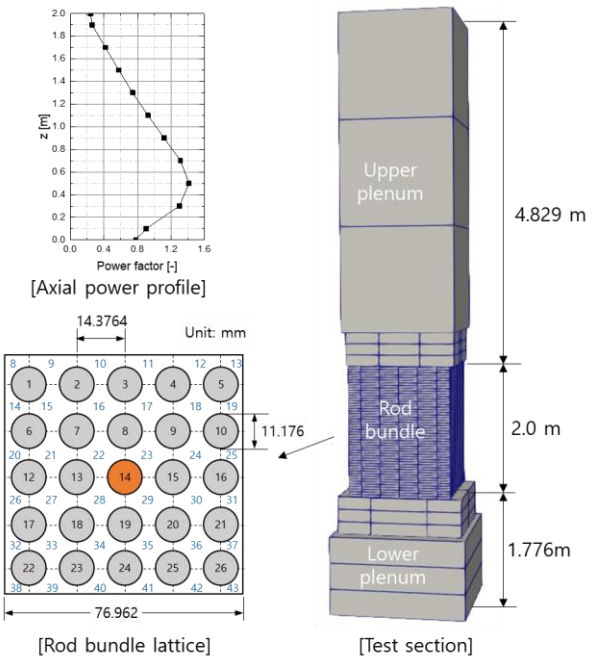

Fig. 2. Conceptual 5×5 rod bundle test

Table 1. Test conditions

#	P [MPa]	$\dot{m}$ [kg/s]	f_z	wall	spacer
1	15.55	10.6–2.12	N	x	x
2			N	o	x
3			U	x	x
4			N	x	o
5	10.92	10.6–2.12	N	x	x
6	8.55		N	x	x

Six cases of different flow conditions, uniform (N) or non-uniform (N) heating method, and with (o) or without (x) solid wall/spacer grid were investigated (Table 1). A linear heat rate of 49.63 kW/m and a constant inlet temperature of 294 ℃ were applied to all the cases. At each pressure, the mass flow rate is reduced by 20% every 5 seconds to investigate its effect on the CHF (Fig. 4a). The test conditions were selected based on the SMART condition.

Non-uniform heating was considered by applying a bottom skewed-shaped axial power profile, f_z (Fig. 3), to all the rods. The solid wall was simulated by four unheated wall-type rods attached to the boundary subchannels. The CHF was calculated at each step using the Groeneveld look-up table.

As observed in Fig. 3, the coolant flow is sufficient to remove heat from the rods if the mass flow rate is above 6.36 kg/s (60 %). The coolant temperature increased while the wall temperature was nearly unchanged, and the CHF decreased as decreasing the mass flow rate. However, as further decreasing the mass flow rate the coolant flow became insufficient and the local heat flux reached the CHF which sharply dropped upstream and downstream of the power peak as observed in Fig. 3d for the mass flow rate of 2.12 kg/s and 4.24 kg/s. This is indicated by a significant rise in the wall temperature. The lower mass flow rate resulted in the earlier rise of the wall temperature.

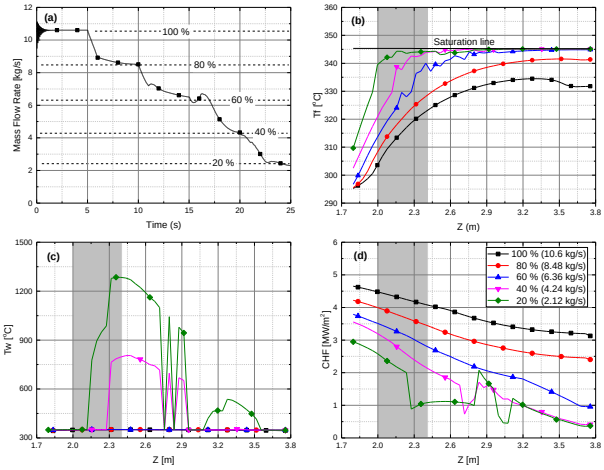

Fig. 3. Effect of mass flow rate on CHF (Case 1)

The peak of the wall temperature is at around the power peak location, not at the exit of the rod bundle (Fig. 3c). The wall temperature fluctuated downstream of the peak due to flow instability and reflooding from the top with the presence of the large unheated water volume. The top reflooding was also indicated by the lower wall temperature near the exit of the rod bundle. It is difficult to determine whether the HN-type CHF condition is reached here. However, the HN heat flux is quite low at 15 MPa (Fig. 1a) to avoid the HN-type CHF occurring.

Figure 4 shows the effect of various factors on the CHF. It is interesting that, among the cases of 15.55 MPa, Case 2 with the presence of the unheated wall showed the lowest CHF at the mass flow rates higher than 6.36 kg/s and the highest CHF at the lower mass flow rates. At the mass flow rate of 2.12 kg/s, Case 2 showed the increase of CHF instead of a decrease as the other cases (Fig. 4e). Also, the highest wall temperature was reached in Case 2 (Fig. 4f). These results were related to the additional pressure drop and additional flow resistance induced by the unheated wall. The higher pressure drop also promoted the flow instability downstream of the power peak and the top reflooding.

Case 3 which considers the uniform heating effect showed the opposite trend of the CHF to Case 2. The CHF curves of Case 3 became separated from the CHF curves of Case 2 downstream of the power peak, and no fluctuations of CHF were observed as in the other cases. Due to the uniform heating, the power supplied to the rods spread over the entire heated length rather than concentrated over the peak region avoiding a sudden rise of vapor generation at a local position. However, the vapor accumulation occurred near the exit of the rod bundle resulting in the high wall temperature in this region (Fig. 4f).

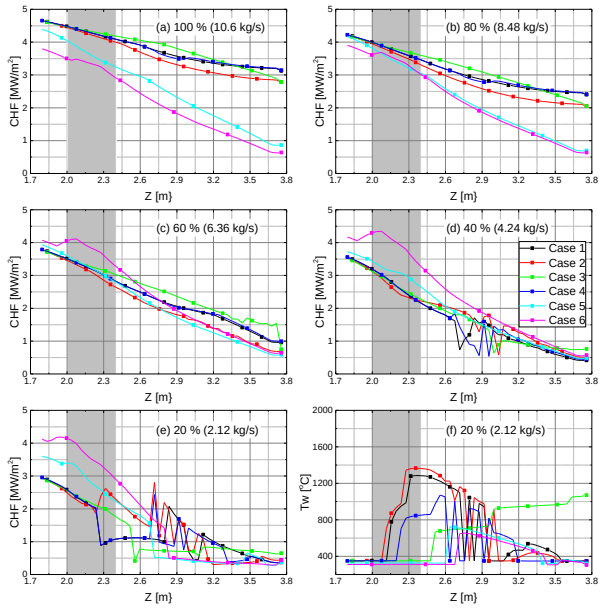

Fig. 4. Parametric effects on CHF

The spacer grid installed at the middle of the rod bundle, which was simulated using an assumed pressure loss coefficient of 0.5, did not show a significant effect on the CHF as observed in Case 4. The CHF curves of Case 4 are quite similar to the default case (Case 1), except for a slight difference in the middle where the spacer grid was installed. However, the wall temperature observed in Case 4 was quite lower in the lower half compared with Case 1. This is because the spacer grid introduced more resistance to the flow, which resulted in a higher pressure in the lower half.

Cases 5 and 6 showed the effect of pressure on the CHF. The lower pressure resulted in the lower CHF at the high flow rates (Figs. 4a & 4b). However, the tendency was reversed, i.e., higher pressure lower CHF, at the lower flow rates (Figs. 4c, 4b, & 4e). The wall temperature in Case 6 of the lower pressure was lower in comparison with Case 5 of the higher pressure. It is quite uncertain about this tendency, no clear explanations for this trend. This is the region of LPLF as mentioned above. Further study on this issue is necessary.

Examination of the calculation results showed a very complex flow field under low flow conditions. The heat transfer regime in the subchannels was single-phase convection and subcooled nucleate boiling (SUBC) at higher flow rates. Then, different regimes were co-existed in a single sub-channel at low flow rates. They are SUBC, saturated nucleate boiling (NB), transient boiling (TRAN), inverted annular film boiling (IAFB), dispersed droplet film boiling (IADF), and dispersed droplet deposition heat transfer (DFFB). The flow regime developed along the subchannel in the order of SUBC–TRAN–IAFF–DFFB–TRAN–SUBC–NB. This indicated the heat transfer regime developed beyond the CHF to transition and film boiling. That explains the fluctuation of the CHF and wall temperature downstream of the power peak.

4. Example LOCA analysis

Considering the LPLP CHF phenomenon in SMRs, the loss-of-coolant accident (LOCA) initiated by a guillotine break at the SI line of the SMART was simulated using the MARS-KS system analysis code.

The analysis was set up based on the limiting case with conservative conditions and assumptions [7]. The calculation results are shown in Fig. 5. Due to the break, the primary side was quickly depressurized and reached the low pressurize pressure (LPP) setpoint of 10.3 MPa causing the reactor trip at 430 seconds. Then, the reactor coolant pumps started to coast down and the control rods were inserted within one second. Consequently, the core power and core flow sharply dropped to nearly zero. The safety injection was also actuated by the LPP signal right after the reactor trip. Hence, the depressurization of the primary size took a longer time, about one hour.

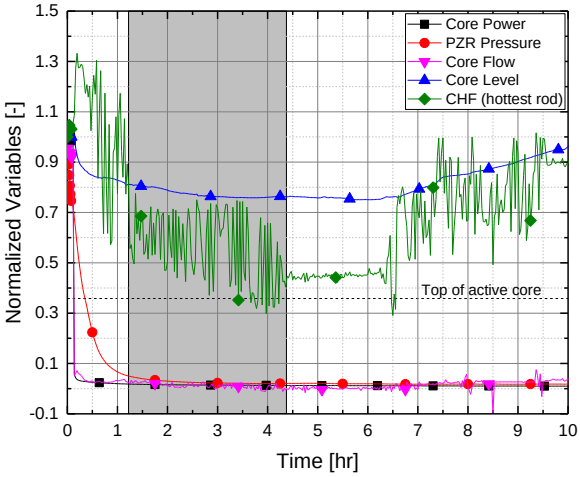

Fig. 5. MARS-KS analysis of SMART LOCA

CHF observation at the hottest rod indicated the remarkable relationship between the CHF value and the flow conditions. There are four clear steps shown on the CHF curve in Fig. 5. Before about one hour, the CHF was high (even reduced) despite the cessation of the core flow. That is because the primary pressure was still

high over this period. Following this period, the CHF reduced to a lower level when the primary pressure was low. After about 4.5 hours, the CHF level remained for two hours and then increased with the recovery of the core coolant level. Specifically, the CHF value significantly fluctuated with respect to the small oscillation of the core flow, which was induced by the water volume in the upper plenum, along the transient. The CHF behavior would be more severe if the safety injection flow is not sufficient to remove the decay heat.

4. Conclusions

The CHF phenomenon in SMR rod bundles is very complicated and influenced by many factors. They are related to the special design of the SMRs, such as non-uniform heating, high power peak, short fuel bundle, spacer grid with mixing vane, and a redundant water column above the core.

The homogeneous nucleation CHF phenomenon which has been concerning for the low-pressure low-flow condition of SMRs was checked, and it showed a low possibility of this CHF type in comparison with the conventional CHF type.

The CHF and wall temperature under the non-uniform heating were opposite to those under the uniform heating condition. The unheated wall and spacer grid showed a slight effect on the CHF. The unheated water volume above the core promoted top reflooding under the low flow condition.

The heat transfer regime complicatedly developed along subchannels under low-pressure low-flow conditions as the heat was not sufficiently removed. In the simulation of SMART LOCA, the CHF passed different regions with a significant fluctuation following the pressure and SI flow behaviors. However, since the decay heat was sufficiently removed, the reactor was brought to the safe shutdown condition. The situation will be serious if the residual heat removal is not sufficient.

Further investigations on the effect of the pressure, flow rate, and even mixing vane on the CHF are necessary. The range of pressure and flow rate should be carefully evaluated so that the used flow condition can reflect the SMR rod bundle CHF phenomenon more adequately.

Acknowledgment

We acknowledge that this research has been conducted with a support from the national nuclear safety research titled “Study on Validation of Consolidated Safety Analysis Platform for Applications of Enhanced Safety Criteria and New Nuclear Fuels (Contract No. 2106002)” funded by Nuclear Safety and Security Commission of KOREA.

REFERENCES

[1] B.W. Yang, H. Anglart, B. Han, and A. Liu, Progress in rod bundle CHF in the past 40 years, Nuc. Eng. Des., Vol. 376, p. 111076, 2021.
[2] B.W. Yang, A. Liu, and B. Han, SMR Rod Bundle CHF-Characteristics and Challenges in Experimental Investigation, NURETH-20, 2023.
[3] B.W. Yang, B. Han, and A. Liu, Low Pressure Low Flow Rod Bundle CHF and Its Challenges in SMR, NURETH-20, 2023.
[4] J.M. Le Corre, S.C. Yao, and C.H. Amon, Two-phase flow regimes and mechanism of critical heat flux under subcooled flow boiling conditions, Nuc. Eng. Des., 240, 245-251, 2010.
[5] W. Liu and H. Nariai, Ultrahigh CHF prediction for subcooled flow boiling based on homogeneous nucleation mechanism, J. Heat Transfer, 127, 149-158, 2005.
[6] D.C. Groeneveld, J.Q. Shan, A.Z. Vasic, L.K.J. Leung, A. Durmayaz, J. Yang, S.C. Cheng, and A. Tanase, The 2006 CHF look-up table, Nuc. Eng. Des., 237, 1909-1922, 2007.
[7] J.H. Chun, B.D. Chung, G.H. Lee, K.H. Bae, Y.I. Kim, Y.J. Chung, and K.K. Kim, Safety evaluation of small-break LOCA with various locations and sizes for SMART adopting fully passive safety system using MARS code, Nuc. Eng. Des., Vol. 277, p. 138-145, 2014.